A novel method to evaluate cleaning quality of oil in shale using pyrolysis pyrogram

Dong, Xu; Shen, Luyi; Zhao, Jianpeng; Liu, Xuefeng; Sun, Yuli; Golsanami, Naser; Wang, Fei; Bi, Haisheng; Zitha, Pacelli

DOI
10.1002/ese3.625

Publication date
2020

Document Version
Final published version

Published in
Energy Science and Engineering

Citation (APA)
Dong, X., Shen, L., Zhao, J., Liu, X., Sun, Y., Golsanami, N., Wang, F., Bi, H., & Zitha, P. (2020). A novel method to evaluate cleaning quality of oil in shale using pyrolysis pyrogram. *Energy Science and Engineering*, *8*(5), 1693-1704. https://doi.org/10.1002/ese3.625

Received: 16 October 2019 | Revised: 6 December 2019 | Accepted: 3 January 2020

DOI: 10.1002/ese3.625

Energy Science & Engineering Open Access

RESEARCH ARTICLE

A novel method to evaluate cleaning quality of oil in shale using pyrolysis pyrogram

Xu Dong[1] | **Luyi Shen**[2] | **Jianpeng Zhao**[3] | **Xuefeng Liu**[4] | **Yuli Sun**[1] | **Naser Golsanami**[5] | **Fei Wang**[1,6] | **Haisheng Bi**[6] | **Pacelli Zitha**[1,7]

[1]College of Electromechanical Engineering, Geo-energy Research Institute, Qingdao University of Science and Technology, Qingdao, China

[2]Department of Physics, University of Alberta, Edmonton, AB, Canada

[3]College of Earth Sciences & Engineering, Xi'an Shiyou University, Xi'an, China

[4]School of Science, China University of Science and Technology, Qingdao, China

[5]State Key Laboratory of Mining Disaster Prevention and Control, College of Mining and Safety Engineering, Shandong University of Science and Technology, Qingdao, China

[6]Department of Oil & Gas Storage and Transportation Engineering, College of Electromechanical Engineering, Qingdao University of Science and Technology, Qingdao, China

[7]Faculty of Civil Engineering and Geosciences, Delft University of Technology, Delft, The Netherlands

Correspondence
Jianpeng Zhao, Xi'an Shiyou University, Xi'an 710065, China.
Email: zjpsnow@126.com

Xuefeng Liu, China University of Petroleum, Qingdao 266580, China.
Email: liuxf@upc.edu.cn

Funding information
National Nature Science Foundation of China, Grant/Award Number: 41804125 and 41874152; Natural Science Basic Research Program of Shanxi, Grant/Award Number: 2018JQ4043

Abstract

Complete and thorough core cleaning is a critical prerequisite for the precise measurements of most rock's petrophysical parameters. In shale, the oil cleaning process, aimed to remove the volatile hydrocarbons, is often complicated by the requirement for intact solid organic. Evaluation of shale's cleaning methods needs to take structural integrity of organic matrix into account but neglected in the existing researches. Here, we develop a novel evaluation method using a modified ESH (extended slow heating) pyrolysis cycle, which starts at a lower initial temperature of 150°C for 10 minutes and then slowly increases to 650°C by 10°C/min. Hydrocarbons on the ESH pyrogram were divided into light free hydrocarbon (S_A), FHR (fluid-like hydrocarbon, S_B), and solid organic matter (S_C). We propose a set of quantitative evaluation criterions comparing the results of pyrograms, for different types of the hydrocarbons, at different cleaning conditions. We showed that a modified pyrogram achieves complete cleaning with S_A and S_B removed while S_C remains almost intact. The modified pyrogram achieves complete removal of FHR in the second stage of pyrogram, while earlier researches often report residual FHR. The introduced method improves the accuracy in the identification of production potential in kerogen-rich shale reservoirs up to about 3% of the total pore volume. Further, the new approach allows a quantitative assessment for the cleaning quality without altering the sample's organic matrix. Future studies on the petrophysical properties of the hydrocarbon-bearing reservoir rocks may benefit from the thorough hydrocarbon removal achieved through the modified pyrogram methods proposed in this study.

KEYWORDS

core cleaning, kerogen richness, modified pyrolysis method, quantitative evaluation, shale

1 | INTRODUCTION

Shale is often the source rock for petroleum generation and contains a large quantity of hydrocarbon which recently became exploitable through the advancement of various enhanced recovery techniques.[1-5] Precise determination of the petrophysical properties of shale is critical for hydrocarbon exploration,[1,2] effective reservoir appraisal,[4,5] and recovery optimization.[1,2] Laboratory analysis of the cores extracted in situ or through exposed outcrops can often provide valuable information and analogues. As such, researchers developed various techniques for core analysis aimed to determine the core's porosity,[6-8] permeability,[2,4] fluid saturation and types,[2,4,9] and electrical[10] and magnetic properties.[9] Critically, the pore fluids formerly occupied the pore spaces of the rock matrix at the samples' virgin states, often need to be removed entirely from the rock matrix to allow the establishment of benchmark measurement values essential for the interpretation of the experimental results obtained from the further testing procedures.[1,2,5] Earlier reviews on the laboratory determination of the petrophysical properties of shale(eg, Sondergeld[1,2] and Glorioso[4,5]) have emphasized the critical role played by the pretreatment procedures which allow the complete removal of liquid hydrocarbons from the pore system. However, the existing researches, concerning the pretreatment process, mainly focus on the cleaning techniques,[11,12] and little attention has been paid to the quality of the oil cleaning process in the laboratory.

At the moment of this writing, a general evaluation of the impacts of oil cleaning results on the laboratory measurements still lacks in the existing scientific discussions. In conventional rocks with no organic matter (eg, sandstone), the oil cleaning would usually aim to remove all hydrocarbons, which consist of the entirety of the organic matter in the rock matrix.[13] However, shale often hosts organic compounds some of which show dual fluid and solid characteristics.[7,14] Also, solid organic matter often exists[7,14] in the shales and needs to be preserved during the cleaning process. As such, a proper evaluation method for the quality of core cleaning needs to consider both the completeness of the hydrocarbon removal and the structural integrity of the organic matrix. The fluorescence detection method, widely used in the conventional rocks, shows advantages in determining the existence of hydrocarbon residuals but is incapable of differentiating the solid phase from the fluid hydrocarbons in the shale.[7,13] Similarly, the nuclear magnetic resonance and particle density comparison methods both suffer from this problem and can results in potentially more significant error than that of the fluorescence detection method.[9,15]

An accuracy examination, calibrating parameters measured after cleaning, can typically be conducted by repeating the same tests or making comparisons with different methods.[2,5,16] Considering that all solid organic matter might have been dissolved in the cleaning process, the petrophysical parameters calculated from these methods or repeated tests should be in high consistency.[2,17,18] However, such comparative approach requires the rock matrix to remain at its virgin states through all testing procedures, even during the potentially destructive cleaning process. A lack of methods to assess the cleaning quality could substantially weaken the testing result's reliability and credibility.[5] Here, we consider a standard Rock-Eval pyrolysis which is frequently used on shale to evaluate the content, origin, and maturity of the organic matter.[19-21] Kuila[7] proposed a method to evaluate the cleaning quality of shale using the Rock-Eval II pyrolysis pyrogram and indicated the disappearance of S1 peak on the pyrogram as the conclusion of the cleaning process. This method solves limitations in the aforementioned methodologies to some extent. Nevertheless, previous research works have indicated that the conventional/basic Rock-Eval II pyrogram has problems in differentiating free hydrocarbon and solid organic matter components in shale.[14,22] Consequently, unreliable cleaning data will be provided when using the basic pyrolysis cycle to evaluate the cleaning quality of hydrocarbons in shale. Since the works mentioned above have failed to properly address the cleaning quality of hydrocarbons in shale, looking for an appropriate method is of inevitable importance.[2,5,7]

In this study, a series of pyrolysis tests were conducted on shale samples at different cleaning conditions. We described an improved ESH (extended slow heating) pyrolysis cycle which is much better than the "basic" Rock-Eval II in dividing hydrocarbon compounds. The main objectives of this study were to (a) illustrate the characteristics of the "basic" and "modified" pyrograms to classify the samples into distinct groups; (b) analyze the effects of pyrolysis modes on characterizing the uncleaned sample's hydrocarbon components in different groups; and (c) discuss the evaluation criterions for characterizing the cleaning progress of a sample to develop a systematic method for evaluating the cleaning quality in shale rocks. The researchers of the current study expect this new approach to quantitatively reveal the cleaning quality of hydrocarbons in the shale without imposing any unwanted changes to the organic matrix. The obtained results from it will bring essential impacts for the petrophysical researches concerning hydrocarbon recovery or precise determination of the rock's petrophysical properties.

2 | EXPERIMENTS

2.1 | Shale rock samples

Shale rock samples used for the cleaning quality examination were collected from the Longmaxi Formation of the Sichuan Basin, southwest of China. The major physical and

TABLE 1 Kerogen type, porosity, bulk density, and TOC of the selected shale samples (R-E II, Rock-Eval II; Rel. diff., relative difference; and Abs. diff., absolute difference)

		Porosity (%)				Density	TOC
Sample	Kerogen type	R-E II	ESH	Rel. diff.	Abs. diff.	g/cm^3	wt%
K-1	II	7.49	7.72	2.98	0.23	2.47	2.213
K-2		5.29	5.41	2.22	0.12	2.57	4.891
K-3		7.28	7.33	0.68	0.05	2.48	3.323
K-4		8.78	9.01	2.55	0.23	2.42	1.178
K-5		6.32	6.46	2.17	0.14	2.48	1.645
K-6		5.43	5.53	1.81	0.10	2.57	1.814
K-7		3.57	3.63	1.65	0.06	2.67	0.921
K-8		5.17	5.22	0.96	0.05	2.47	1.569
K-X		6.25	6.25	–	–	2.45	0.172

geochemical parameters of the samples are listed in Table 1 for kerogen type (II), porosity, bulk density, and total organic carbon (TOC). Samples at mesh size of 60-70 were used in the cleaning process. The porosities were measured for the aliquots that cleaned under two different criterions using the Rock-Eval II pyrogram and the ESH pyrogram. While the ESH-related porosity was in the range of 3.63%-9.01%, the relative differences between the two measured porosities ranged in 0.68%-2.98%. The bulk density fell in the range of 2.42-2.67 g/cm^3. The collected data showed that the TOC values in the samples were 0.172-4.891 wt%.

2.2 | Component model

A component model was built to accomplish the desired cleaning target of this study as shown in Figure 1. The matrix of the shale was classified into the organic matrix and the inorganic matrix.[23,24] The former part mainly consisted of the primary kerogen and solid bitumen. The volume percentages of the kerogen and solid bitumen included both the hydrocarbons generated from pyrolysis and the residual organic carbon components of any primary kerogen, solid bitumen, and detrital organic matter.[21] The inorganic matrix on the other hand was the dry clay particles and the nonclay grains (ie, quartz and feldspar).[6] Since under in situ conditions, fluids typically occupy the pore space of the rock matrix, researchers have generally considered porosity to be equal to the ratio of rock matrix occupied by the fluids against the total rock matrix volume.[5,7] In Figure 1, the whole pore space ($V_{p\text{-}total}$) is filled with water and nonsolid hydrocarbons. The water is composed of three types, namely free water, clay bound water, and capillary bound water. The nonsolid hydrocarbon was our cleaning target which should have included all hydrocarbons existing in gas, liquid, and semiliquid form. In the model, the nonsolid hydrocarbons are finely divided into light free hydrocarbons and FHR (fluid-like hydrocarbons residue) via the characterizations of organic matter fractions in unconventional tight reservoirs.[14,22] The FHR, naturally, often consists of heavy volatile hydrocarbons.[14,22] More information on this issue will be provided in the discussion section. Generally speaking, all original fluids need to be removed entirely from the pore space prior to doing a proper matrix determination experiment. The cleaning of hydrocarbons in our shale samples was to remove all the nonsolid hydrocarbons. Consequently, the targets in the process were light free hydrocarbons and FHR, but the kerogen and the solid bitumen were to be excluded.

2.3 | Pyrolysis concepts

During the Rock-Eval pyrolysis cycle, a fragmented rock sample (about 100 mg) is heated through an inert atmosphere of helium (or nitrogen) with a programmed temperature. A flame ionization detector (FID) senses volatile compounds emitted during each process of heating. Spectroscopies of CO and CO_2 are measured using sensitive infrared detectors during pyrolysis. Temperatures in the pyrolyzer are typically monitored through thermocouple. These measurements are

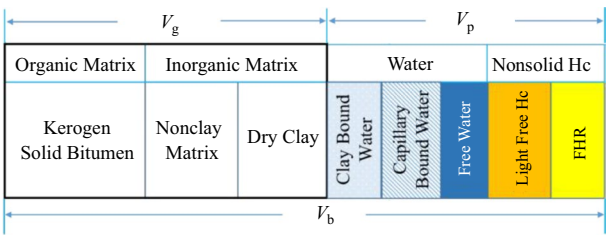

FIGURE 1 A conceptual model for material components of shale. V_g represents the volume of the grain skeleton of the specimen, and V_p shows the pore spaces. Yellow and orange colors denote the cleaning target of study (nonsolid hydrocarbons)

charted as the commonly known pyrogram. The pyrogram produced in the process would help researchers identify the type and maturity of organic matter in sediments and characterize the thermal evolution of the sample and its residual hydrocarbon-generating potential.[25,26] The fundamental concepts of the "basic" and "modified" pyrolysis techniques will be introduced in the upcoming section.

The "basic" Rock-Eval II is a rapid pyrolysis technique. During the cycle, the aliquot is heated using a programmable temperature controller in the pyrolyzer.[25] The pyrolysis stages begin with a heating period of 3 minutes with a constant temperature of 300°C (S1 stage), followed by temperature increase to a peak value of 650°C at a rate of 25°C/min (S2 stage).[25] The amount of hydrocarbon (mg HC/g Rock) released during the pyrolysis stage is measured between S1 and S2 peaks. Programmable temperature follows Equation (1) as:

$$T = \begin{cases} 300 & (t \le 3) \\ 25\,(t-3)+300 & (3 < t \le 17) \end{cases} \quad (1)$$

ESH pyrolysis technique, a modified extended slow heating pyrolysis method,[14,22] begins with an initial temperature of 150°C and the fragmented sample is held for 10 minutes. The next stage is to increase the heating temperature by a step size 10°C/min (which is much slower in comparison with the basic cycle) until up to 650°C. The pyrogram is expressed by a series of peaks which include S_A, S_B, and S_C.[14,22] The programmable temperature follows Equation (2). The detailed meanings about the three parts on the ESH pyrogram will be explained in the discussion part of the current paper.

$$T = \begin{cases} 150 & (t \le 10) \\ 10\,(t-10)+150 & (10 < t \le 60) \end{cases} \quad (2)$$

2.4 | Procedures

The procedure for the current study mainly consisted of two parts: sample treatment and cleaning quality evaluation. The designed flowchart for the cleaning of hydrocarbons in the shale is shown in Figure 2 where the rinsing and extraction were the key parts for sample treatment process. Rinsing prior to extraction aims to eliminate the parasitic ionization effect on pyrolysis analysis. Usually, only one rinsing is enough but the operation could be duplicated if needed. Another advantage of rinsing aliquot is for the Rock-Eval apparatus itself. The presence of salts (eg, chloride and sulfate) causes damage during the oxidation phase, in particular on the piston of furnace, thermocouple, and crucibles, which all would get corroded.[27] Herein, the widely used core cleaning method, distillation extraction method (Dean-Stark),[13] was adopted to remove the free hydrocarbons because it is

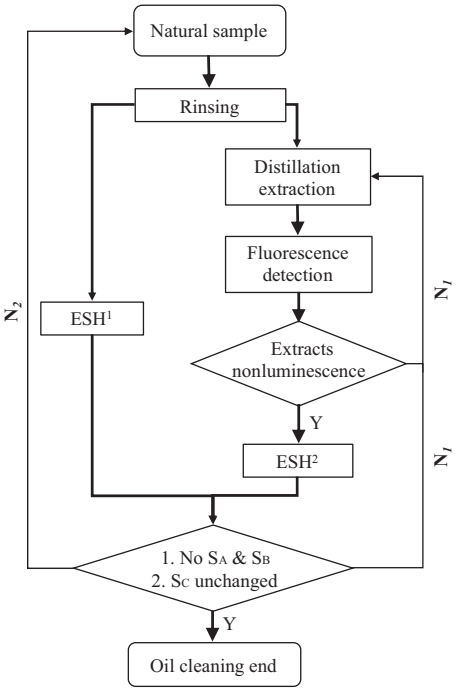

FIGURE 2 Experiment flowchart of hydrocarbons cleaning. Thickened arrows represent the main steps for each iteration. Thin-arrows indicate the repetitive steps

efficient in extracting target components and can provide a purifying result.[28] A proper solvent is critical to remove original fluids properly. Since solvents have different properties, a specific solvent might be preferred to ensure cleaning efficiency for certain applications. Mixed solvents are generally required to extract hydrocarbons with different molecular structures.[13] Therefore, an optimized style and proportion of solvents are recommended based on the regional oil analysis data and expert experiences. In the case of the current research, methylene chloride and acetone (3:1) were used in the procedures. Meanwhile, two main techniques, for example, the fluorescence detection and the modified ESH pyrolysis method, were used for the evaluation of the cleaning quality at different stages. The former technique was manipulated for a prejudgment of the cleanliness of the samples at the early stage of the cleaning process. The second technique, however, was applied for a quantitative evaluation of the cleaning quality at the latter stage. The cleaning quality was evaluated by making a comparison on the pyrograms measured at the uncleaned (before cleaning) and cleaned (after cleaning) conditions. All pyrolysis measurements were subsequently processed in the Rock-Eval VI pyrolyzer. The following represents the detailed procedures as shown in Figure 2.

1. Powder the uncleaned sample to about 60-70 mesh, which has proven not to alter the integrity of the grain-size composition in shale during crushing.[8] Rinse the crushed aliquots with deionized water prior to extraction.

2. Evacuate the air in the pyrolyzer system and preset parameters for the pyrolysis analyzer according to the ESH mode. Then, heat at 150°C for 10 minutes and consequently go up to 650°C by the step sizes of 10°C/min.
3. Collect some of the rinsed and uncleaned sample to obtain the pyrogram and define it as ESH^1.
4. Start cleaning with distillation extraction method (methylene chloride:acetone = 3:1).[29]
5. Prejudge the extraction quality of the sample with a fluorescent detection method. Nonluminescence of the extract under a fluorescent light is a good criterion for determining the cleanliness of the oil.[13] Repeat the step until approximately no oil luminescence is found in the extracts. Otherwise, the aliquot needs another cleaning cycle following N_1, which means a new cycle is needed because not all volatile hydrocarbons have been extracted.
6. Collect the extracted aliquot to derive the ESH pyrogram and define it as ESH^2.
7. Evaluate the cleaning quality of hydrocarbons according to comparison results between ESH^1 and ESH^2.
8. Cleaning ends if the quality evaluation criterions are met. Otherwise, the cleaning failed and the cleaning aliquot should be abandoned following N_2, because the organic matrix in the sample is altered.

3 | RESULTS AND DISCUSSION

Rock-Eval pyrolysis techniques have been widely used for assessing the quality, quantity, and maturity of hydrocarbons associated with source rocks.[30] However, it is a novel solution to evaluate the cleaning of hydrocarbons in shale by using the pyrolysis pyrogram. Since the progressive pyrolysis cycle has problems in differentiating fractions of hydrocarbons in the reservoir, in the current research, the modified ESH pyrolysis mode was utilized to evaluate the cleaning quality.[14,22] To simplify the analysis process, samples were classified into two distinct groups according to the morphology of the ESH pyrogram. The characteristics of the Rock-Eval II and ESH pyrograms are discussed first to show their significant differences in the characterization of hydrocarbons' components. Subsequently, the evaluation criterions for the cleaning quality of hydrocarbons through the modified technique are discussed for providing a clear and universal standard that can be used on samples with different properties. Finally, a comparison is conducted on porosities measured on aliquots treated under different criterions derived from the two pyrolysis modes to show their impacts on reservoir evaluation.

3.1 | Difference of pyrograms for kerogen-rich shale

Figures 3-5 show the Rock-Eval II pyrogram and ESH pyrogram measured for three typical shale samples before cleaning. These pyrograms are characterized by a bimodal to unimodal change of the S2 peaks. The types of released hydrocarbons are illustrated by a series of peaks on the controlled heating pyrogram. Since the samples in this section generally showed two or three peaks and released

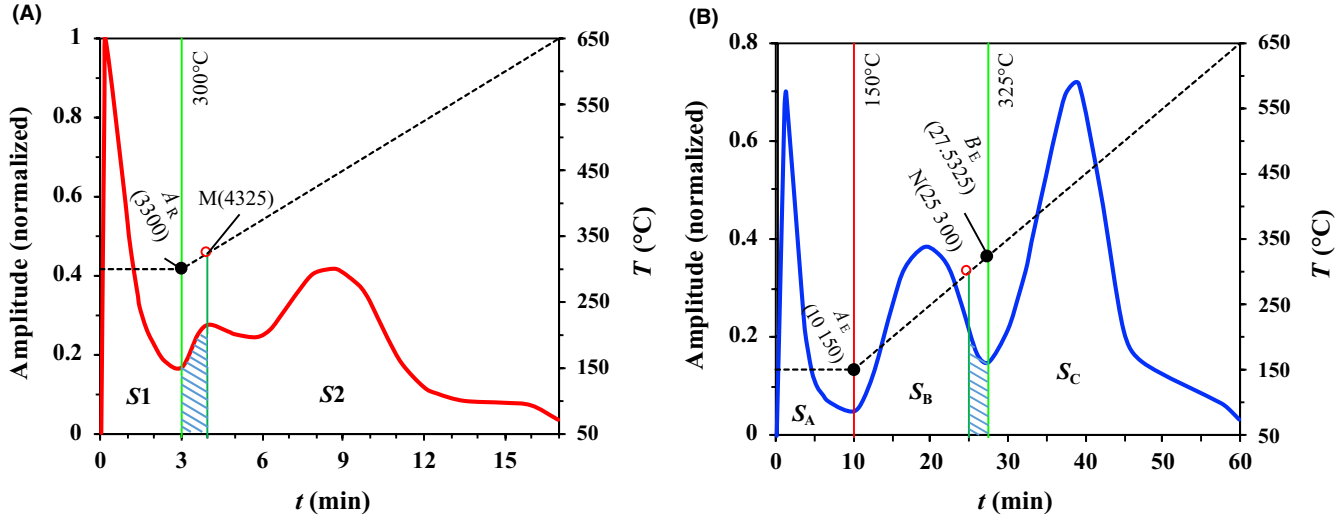

FIGURE 3 Hydrocarbon cleaning results for the kerogen-rich shale K-1 using Rock-Eval II pyrogram (A) and ESH pyrogram (B). The S2 peak shows a bimodal structure and is characterized by a smaller peak followed by a more prominent broad peak. Red curve in (A) represents the Rock-Eval II curve divided into zones of S_1 (300°C) and S_2 (greater than 300°C). Blue curve in (B) shows the pyrogram curve for S_A (150°C, light free hydrocarbon), S_B (between 150°C to 325°C, FHR), and S_C (greater than 325°C, solid organic matter). Dashed black line shows the temperature history. Shaded zones represent the uncleaned FHR in Rock-Eval pyrogram

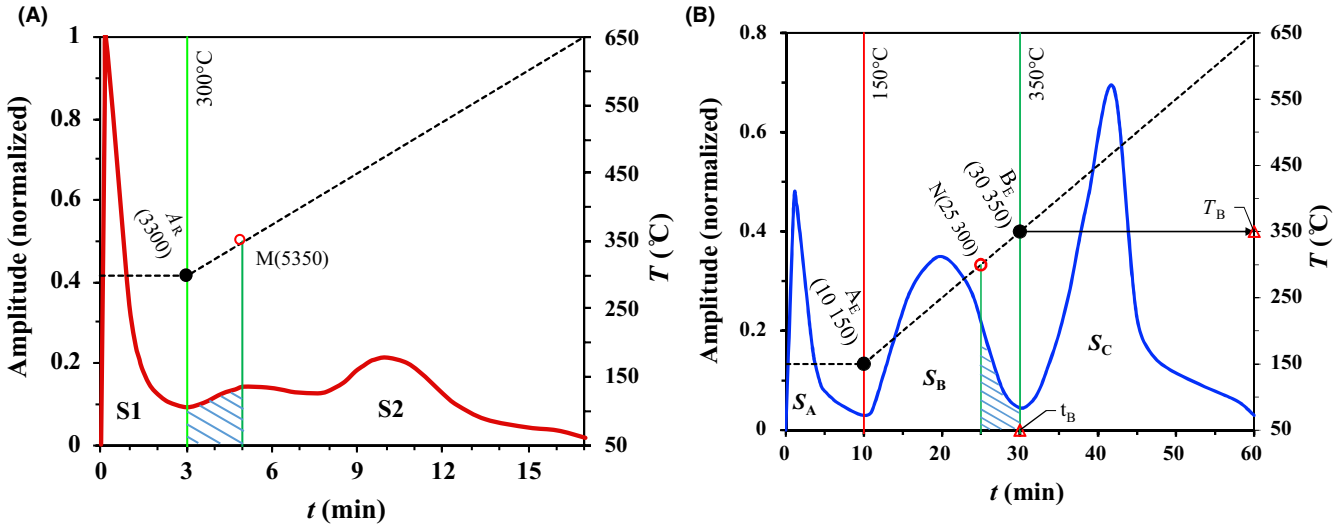

FIGURE 4 Hydrocarbon cleaning results for the kerogen-rich shale K-2 using Rock-Eval II pyrogram (A) and ESH pyrogram (B). The S2 peak shows a poorly bimodal structure and is characterized by a smaller peak with weak amplitude change followed by a more prominent broad peak

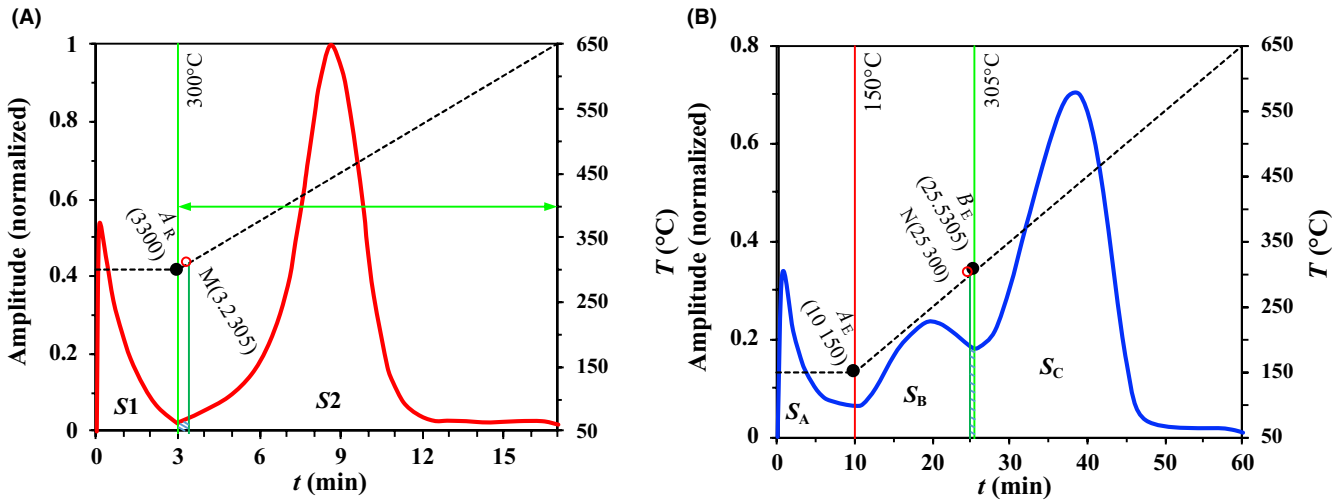

FIGURE 5 Hydrocarbon cleaning results for the kerogen-rich shale K-3 using Rock-Eval II pyrogram (A) and ESH pyrogram (B). The S2 shows a unimodal structure

large hydrocarbons on the S_C peak of the ESH pyrogram, we grouped them as the kerogen-rich (prone) shale. Take K-1 as an example, the *x*-axis refers to the heating time with 17 minutes and 60 minutes for the two cycles in Figure 3. The primary *y*-axis shows the amplitude of hydrocarbons released during each pyrolysis stage, which is normalized according to the maximum amplitude of the two pyrograms. The secondary *y*-axis represents the heating temperature, where the former cycle ranged at 300-650°C, and the latter one was at 150-650°C. The characteristics and significant difference between the two kinds of pyrograms are discussed in sequence.

The Rock-Eval II pyrogram and its heating mode of K-1 are, respectively, shown in red solid line and dotted line in Figure 3A. The amounts of different hydrocarbons released during the pyrolysis stages were measured between S1 and S2. The solid division (green vertical solid line) between S1 and S2 always passes vertically through point A_R (3 minutes, 300°C). The S1 stage, which mainly responded to the free oil and the gas previously generated by the bitumen, represents free hydrocarbon components that evolve from the rock sample without cracking the kerogen during the heating at 300°C in 3 minutes.[28] In this cycle, the hydrocarbons were generated in the subsurface but can only be expelled from the rock during pyrolysis.[24,27] The S2 stage involves the pyrolysis of more durable organic matter fractions and releases hydrocarbons along with carbon dioxide and monoxide. The released hydrocarbons were the results of the cracking of heavy hydrocarbons and the thermal breakdown of kerogen.[31]

In the Rock-Eval VI technique, the maximum temperature can be extended to 850°C to obtain the inorganic carbon content.[27] Since the part between 650 and 850°C did not fall in the scope of the current research and the Boudouard reaction could be prevented below 650°C,[32] herein, the programmed maximum temperature was not extended beyond 650°C in this paper. Different temperatures, for example, 100°C,[33] 150°C,[14,22,30] 180°C,[28,34,35] 200°C,[36,37] and 300°C[7,25] are found as the initial heating temperature in the pyrolysis analysis for different uses. A lower initial temperature can prevent the decomposition of the most labile components of the organic matter and ensures that only the lightest fraction of free hydrocarbons are volatilized.[27] 10°C/min,[14,22,30] 25°C/min,[7] and 30°C/min[28,36] are generally conducted at the second pyrolysis stage. According to the research studies on organic matter fractions in unconventional tight reservoirs, a longer pyrolysis process could result in a fine evolution of different fractions of organic matter.[14,22,30] Therefore, the ESH cycle, which starts at a lower temperature of 150°C with a lower step size of 10°C/min to 650°C, is conducted to resolve different fractions of hydrocarbons in the tight reservoir rocks.[14]

The ESH pyrogram and its heating mode of K-1 are, respectively, shown in blue solid line and dotted line in Figure 3B. The stage is characterized by the three peaks, say S_A, S_B, and S_C. The main components in the three fractions have proven to be light free hydrocarbons, FHR, and solid organic matter, respectively.[14,22,30] The two vertical lines at points A_E and B_E divide the ESH pyrogram into the three fractions. The vertical division at A_E (red solid vertical line) always locates at $t = 10$ minutes and is the solid (first) division between S_A and S_B. The division between S_B and S_C can be determined with the trough between them, which will change with the property of organic matters in different samples.[22] The vertical line at B_E (green-solid vertical line) shows the second division for K-1. Followings are the steps to calculate the parameters of B_E (t_B, T_B): First, find the trough between the second wave and the third wave. Second, draw a line parallel to the *y*-axis that intersects heating line, trough, and *x*-axis. The intersection at the *x*-axis is t_B, and the intersection with the heating line is point B_E. Third, draw a line parallel to the *x*-axis from B_E to the secondary *y*-axis. Finally, the point where it intersects the secondary *y*-axis is T_B. For K-1, $t_B = 30$ minutes and $T_B = 350$°C. The B_E for K-2 (Figure 4B) and K-3 (Figure 5B) was (27.5, 325) and (25.5, 305), respectively. In short, T_B was the cut off heating temperature for the complete volatilization of all free hydrocarbons that existed in gas, liquid, and semiliquid forms.

Compared with the "basic" cycle, the modified technique provides a more sufficient pyrolysis time, lower heating rate, and lower initial temperature. The S_A fraction at the lower isotemperature of 150°C shows the volatilized light free hydrocarbons (including light oil and gas condensates) that were trapped within the rock. The gas chromatography results showed that the hydrocarbons released roughly corresponded to below C9-C10.[14] The second peak, S_B, represents the FHR (fluid-like hydrocarbons residue) and is evolved at the approximate pyrolysis temperature range of about 150-350°C. At this range, the majority of the remaining organic matters were medium to heavy range hydrocarbons (roughly C10-C20) in the forms of semiliquid and liquid.[14,22] To be more specific, these organic matters were fractions of higher molecular free hydrocarbons. Naturally, they exist in the form of film of condensed, heavy molecular hydrocarbon residues coating on surfaces of the intergranular pores, and solid organic matter.[14,22,30] The FHR can be observed with photomicrographs under white incident light by 50-times objective.[14,22,30] The S_C generally ranged at about 350-650°C and consisted of hydrocarbons generated from solid organic matter including remnant primary kerogen, solid bitumen, and refractory and detrital organic matter.[22]

In morphology, the traditional S1 and S2 components in the Rock-Eval II pyrogram are modified into three finer peaks: S_A, S_B, and S_C.[14] Besides the morphology of pyrograms, the shaded regions (approximately same in area) that, respectively, appeared on the two pyrograms of Figures 3-5, were the most significant difference in components' classification for the two pyrograms. Two auxiliary vertical lines that pass through two special points (M and N) are introduced to explain the difference between the two pyrograms. M on the Rock-Eval II pyrogram has the same threshold heating temperature (T_B) with B_E. Point N on the ESH pyrogram shares the same heating temperature with A_R on the Rock-Eval II pyrogram, which is 300°C. The shaded regions on the two pyrograms, A_R-M on the Rock-Eval II pyrogram and N-B_E on the ESH pyrogram, have the same range of temperature, for example, 300-325°C for K-1 (Figure 3), 300-350°C for K-2 (Figure 4), and 300-305°C for K-3 (Figure 5). The shaded region represents a part of the FHR on the ESH pyrogram that will be interpreted as the sold organic matter because it shows up on the second stage of the Rock-Eval II pyrogram. The ESH pyrogram of the kerogen-rich sample generally has three distinct peaks and shows apparent amplitude changes among peaks. In K-1, the S2 shows a better bimodal structure and is characterized by a smaller narrow peak followed by a more prominent broad peak, where the left board shoulder falls at 3-6 minutes (300-375°C) and the following broad shoulder shows at 6-17 minutes (375-650°C) (Figure 3). The S2 for K-2 shows a poorly bimodal structure and is characterized by a smaller broad left shoulder before 8 minutes (300-425°C) followed by a broad shoulder observed after 8 minutes (425-650°C). The S2 peak on the corresponding Rock-Eval II pyrogram usually shows a bimodal structure (eg, Figures 3 and 4). However, approximately no obvious amplitude changes were found around the trough, which is the common characteristic shared in this kind of sample. As the shaded region shown on the left part of Figures 3 and 4,

the left shoulder of the smaller peak on the S2 (eg, 3-4 minutes for K-1 and 3-5 minutes for K-2) represents the part of FHR that was not fully released in the first stage of the Rock-Eval II. In other words, the unshaded region on FHR, which represents the majority of FHR, was released in the first stage of the basic cycle. The other regions shown on S2 were released from the pyrolysis of kerogen.[14] In K-3, the shaded region has a very small temperature range. The vast majority of the FHR is volatilized in the first stage which could explain why no shoulder shows on the unimodal structure of S2 (Figure 5A). Clearly, for the kerogen-rich shale samples, the higher initial isotemperature (300°C) in the Rock-Eval II cycle can volatize the total light free hydrocarbons and the majority of FHR, simultaneously. But the residual FHR will be regarded as a solid organic matter. As conclusion, the FHR that remained to the second stage of the Rock-Eval II cycle is the most noticeable difference between the modified pyrogram and basic pyrogram. The shaded region reflects the error interval using the Rock-Eval II pyrogram instead of ESH pyrogram to classify the FHR and solid organic matter in the kerogen-rich samples.

3.2 | Difference of pyrograms for kerogen-poor shale

The Rock-Eval II and ESH pyrograms of uncleaned sample K-X are represented in Figure 6. As no hydrocarbons were released at the S_C stage, we grouped this kind of sample as the kerogen-poor (prone) shale. Axes and the fraction division A_R are the same as in Figure 3. The division at B_E shows a subtle difference with the kerogen-rich sample. The Rock-Eval II pyrogram generally had one continuous S1 peak and no S2 fraction. The ESH pyrogram changed to a bimodal structure characterized by S_A followed by S_B in morphology. Besides the morphology, S_B is the most noticeable difference between the ESH pyrogram and the Rock-Eval II pyrogram of the kerogen-poor sample. In Figure 6B, the light free hydrocarbons were volatized at 150°C in the beginning 10 minutes. Moreover, FHR was totally released when T_B is equal to 210°C. In short, all free hydrocarbons that existed in gas, liquid, and semiliquid forms in sample K-X can be completed volatized at 210°C.

Significant heterogeneity usually exists in shale,[38] and the organic abundance of shales differs from each other significantly.[39,40] During the hydrocarbon generation process, due to the hydrocarbon-generating overpressure effect,[41,42] the pressure in the kerogen-rich shale will increase. However, the pressure in kerogen-poor shale will remain unchanged since there is no hydrocarbon-generating capacity in it. As a result, oil/gas will migrate from kerogen-rich shale to the adjacent kerogen-poor shale under the drive of pressure gradient.[43] Due to the fact that there is some oil/gas but no other components in the Rock-Eval pyrogram of the kerogen-poor shale, only S1 peak but no S2 peak can be detected in the pyrolysis experiments (Figure 6A). Note that S1 represents free oil and gas, and S2 indicates the hydrocarbons generated from the cracking of heavy hydrocarbons and the thermal breakdown of kerogen. The Rock-Eval pyrolysis mode gives a blurred division of components on the pyrogram. Nevertheless, the ESH pyrogram (Figure 6B) clearly reveals that no hydrocarbons were generated from the thermal breakdown of kerogen (S_C peak). Besides the volatilized light free hydrocarbons (S_A), there also existed a number of higher molecular hydrocarbon residues (S_B) on the ESH pyrogram. On the one hand, the lacking of any peak between 210 and 650°C on ESH pyrogram (Figure 6B) suggested extremely mature organic matter with no pyrolysable components in the studied source rock. On the other hand, the kerogen-poor sample (K-X) in this study could be expressed as non-source-prone rock much like mudstone.[14] As a conclusion, all free hydrocarbons can be volatized when the heating temperature gets over T_B. What's more, heating within 650°C does not alter any solid organic matter framework in this kind of samples.

3.3 | Quality evaluation criterions

The particularity of organic matter in shale indicates that all light free hydrocarbons and FHR are required to be completely removed, but the kerogen and the solid bitumen should be maintained in the hydrocarbons cleaning process.[14,22,30] For the two sets of samples, ESH pyrograms measured at different cleaning conditions will be separately compared in this section to clarify the evaluation criterions of the cleaning quality. Since the fluorescence detection method is incapable of differentiating the solid phase from the fluid hydrocarbons in shale, using it will pose additional risks of dissolving all or part of solid organic matter. Therefore, the method was merely employed to prejudge the cleaning effect in the early stage of the process (Figure 2). Nonluminescence of extract under fluorescent light indicated no obvious hydrocarbons were extracted. After that, the ESH pyrolysis test was conducted on the cleaned aliquots. The prejudgment method can help to avoid the blind conducting of ESH tests so as to improve the testing efficiency.

Three ESH pyrograms measured at different cleaning conditions of the kerogen-rich sample K-1 are illustrated in Figure 7. The blue solid line and the red dashed line represent the pyrograms measured before cleaning and after cleaning, respectively. The dashed-dotted line (black) shows a pyrogram measured during the cleaning process. As noted in the former sections, the targets in the cleaning process for the sample were S_A and S_B, but the S_C would be left out. Therefore, for the kerogen-rich shale samples, which are similar in morphology with the ESH pyrogram of K-1, the disappearance of fractions on the

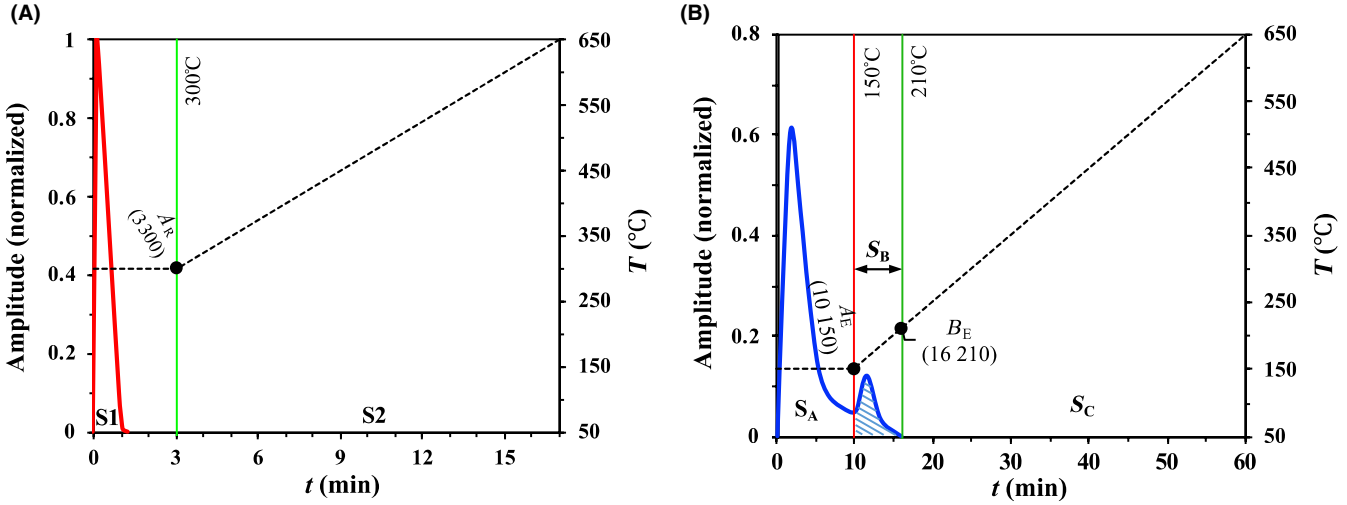

FIGURE 6 Hydrocarbon cleaning results for the kerogen-poor shale K-X using Rock-Eval II pyrogram (A) and ESH pyrogram (B)

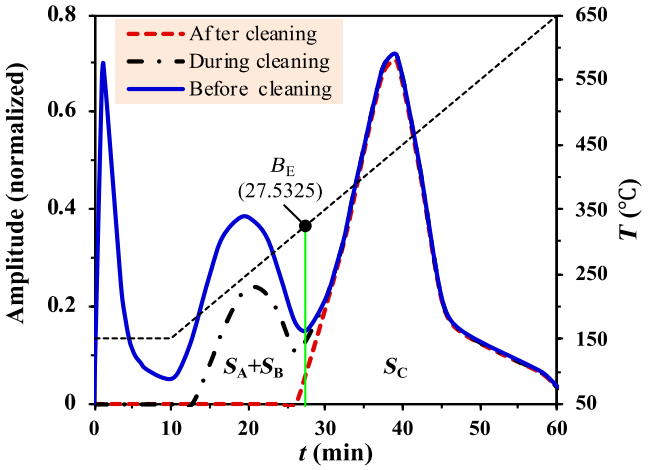

FIGURE 7 ESH pyrograms of kerogen-rich sample K-1 measured at "before cleaning," "during cleaning," and "after cleaning" status. Thin dashed black line represents the temperature history. Black dots B_E represent the threshold value for complete cleaning

left side of the division B_E implies that the light free hydrocarbons together with the FHR are removed. The (approximately) invariance of the S_C fraction implies that the solid organic matter matrix was intact. The cleaning is completed when the result shows an ESH pyrogram like the one shown in "after cleaning" condition. If the pyrogram is like the one "during cleaning," that means the sample needs a new cleaning cycle because not all the free hydrocarbons have been removed. The alteration of the Sc fraction implies that the structural integrity of the solid organic matter in the matrix is destroyed and the cleaning has failed. Under such a condition, all the following matrix characterization results can be unrepresentative, as the rock matrix has already been altered in the process of core cleaning. In addition, the obtained three ESH pyrograms of the kerogen-rich sample showed distinct variation on amplitude and fractions. The changing of the pyrograms with the cleaning cycles proves that in the distillation extraction process, the heavier hydrocarbon fraction is harder to be extracted than the lighter fraction. Therefore, dissolving solid organic matter in the cleaning process could be avoided when using the ESH pyrolysis criterions to evaluate the cleaning quality of hydrocarbon in the shale. In summary, the hydrocarbon cleaning evaluation criterions for the kerogen-rich-prone shale samples are concluded as follows: (a) Cleaning is achieved when S_A and S_B disappeared and S_C is almost unchanged on the ESH pyrogram; (b) continue to clean if S_B remnants are observed; and (c) cleaning failed if S_C shows obvious absence.

The impact of using Rock-Eval II pyrogram to evaluate the cleaning result is obvious. In the conventional evaluation method, the disappearance of S1 in the Rock-Eval II pyrolysis pyrogram was regarded as the end of the cleaning process for the shale.[7] The cleaning process failed as the disappearance of (or part) S2 was observed on the cleaned sample's pyrogram.[7] Obviously, using the method would introduce a huge error, because of the part of FHR (shaded region shows at the second stage of S2) will be kept as the solid organic matrix in the cleaning-completed sample. The disappearance of a part of S2 could be resulted by a portion of the FHR components in S_B but not the real solid organic matter in S_C. For instance, the free hydrocarbons in the ESH cycle of K-1 (Figure 3B could be completely volatilized when raising the temperature up to $T_B = 325°C$. In Figure 3A, this temperature T_B appears at the fifth minute. Therefore, the deduction could not be supported if the dissolved part just covered the shaded region A_R-M. Obviously, the progressive pyrolysis mode makes the conventional Rock-Eval II pyrogram incapable of effectively evaluating the cleaning quality. The former studies could have been more realistic if they had considered the FHR in the organic matter.[7]

Figure 8 shows the ESH pyrograms measured for the kerogen-poor sample K-X at two different conditions. The blue solid line represents the pyrogram measured before cleaning.

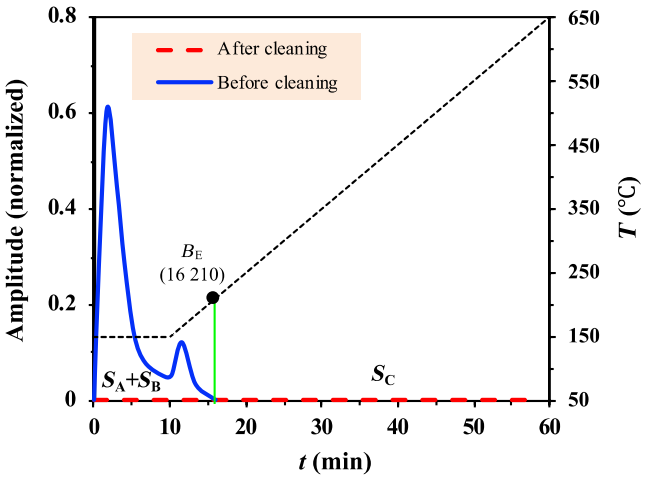

FIGURE 8 ESH pyrograms of the uncleaned and cleaned kerogen-poor shale sample K-X

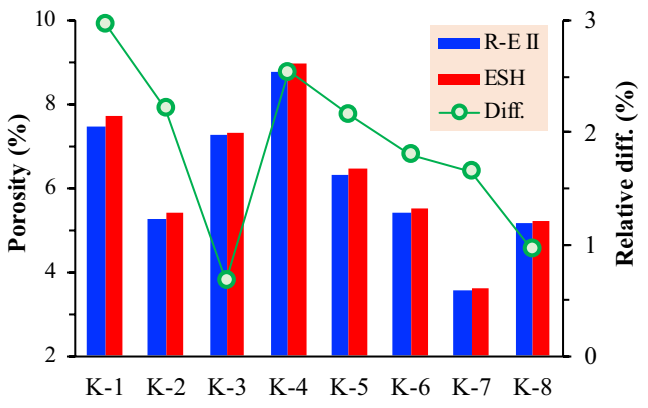

FIGURE 9 Porosities measured for the cleaned kerogen-rich aliquots by following the cleaning criterions of the Rock-Eval II pyrogram (blue) and ESH pyrogram (red). The circles represent the relative difference of the two porosity values

The pyrogram obtained after cleaning is shown in red dashed line, which is zero in amplitude. The sample was characterized by a sole and continuous S1 peak on the Rock-Eval II pyrogram and a bimodal structure on the ESH pyrogram (Figure 6). As no S_C fraction was noticed within 650°C in the ESH cycle, the disappearance of S_A and S_B could indicate the complete cleaning of all the free hydrocarbons. As the heavier hydrocarbon fractions are harder to be extracted than the lighter fractions in the cleaning process, no S_B fraction being left in ESH pyrogram under such condition is effective to verify that the free hydrocarbons were completely cleaned and the matrix is intact. The quality evaluation criterions for the cleaning of kerogen-poor samples are as follows: (a) Cleaning is accomplished if no S_A and S_B fractions show on the ESH pyrogram of the cleaned aliquot; (b) continue to clean if some S_B remnants are observed. Note that in the evaluation of cleaning results, compared with the modified method, using the Rock-Eval II technique could not introduce obvious difference for this kind of samples since the disappearance of S1 has the same meaning as the absence of S_A and S_B.

The foresaid would be concisely summarized as follows: (a) Cleaning is achieved when S_A and S_B disappeared and S_C is almost unchanged on the ESH pyrogram for the cleaned kerogen-rich sample; (b) cleaning is accomplished if no S_A and S_B show on the ESH pyrogram for the cleaned kerogen-poor aliquot; and (c) using the conventional pyrogram to evaluate the cleaning result shows impact mainly on the kerogen-rich samples.

3.4 | Porosity difference

As mentioned above, for the kerogen-rich samples, using the disappearance of S1 instead of S_A and S_B as a criterion to clean the sample will inappropriately maintain the FHR that remained to the second stage of the conventional cycle as the solid organic matter. Evaporative loss of hydrocarbons could happen in the preparation before pyrolysis. The actual volume percentage of the fractions in the hydrocarbons is hard to be derived from the pyrogram.[27] The porosity is strongly affected by the cleaning result and is an important parameter for the estimation of the reservoir production potential. Thus, the porosity of the crushed aliquots will be measured to show the difference between the two different criterions deduced from the Rock-Eval II and the ESH techniques. Since the conventional pyrogram-derived criterion is effective for the kerogen-poor samples, the porosity is discussed only for the kerogen-rich sample.

As the disappearance of S1 happens earlier than that of S_B, the total gas (helium) accessible porosity of the aliquots collected from the extracted crushed sample was measured using the gas injection porosimetry (GIP) method under the two conditions in turn, namely the Rock-Eval II cycle and ESH cycle. The measurements came to a relative error of 0.5%.[8] The well-calibrated porosimetry system would supply grain volume within approximately ±0.03 cm^3 of the true value for the researched aliquots.[13] Prior to porosity measurement, the kerogen-rich aliquot was dried at 200°C for 24 hours to remove all residual pore water and solvents to get a dry matrix.[10,44] The temperature could not produce dehydration of the residual FHR in the Rock-Eval II cycle because it was lower than the threshold temperature T_B. Figure 9 depicts the porosity results measured of the Rock-Eval II criterion (blue) and ESH criterion (red). The circle (green) represents the relative difference of the porosities. For the researched aliquots, the results showed that the porosity values derived with the ESH criterion were larger than that of the Rock-Eval II criterion. The relative and absolute differences of the porosities were, respectively, in the range of 0.68%-2.98% and 0.05-0.23 PU, which are obvious larger than the error provided by the porosimetry method and the apparatus.

Therefore, the interpreted porosity from the two cycles could reflect the error interval when using the Rock-Eval II criterion to evaluate the clean quality in the kerogen-rich shale. In other words, when attempting to evaluate cleaning effect with the conventional pyrogram rather than the modified pyrogram, up to about 3% of total pore volume would be potentially neglected while identifying production potential in the shale reservoirs.

4 | CONCLUSIONS

To quantitatively evaluate the cleaning quality of hydrocarbons in the shale without imposing any unwanted changes to the organic matrix, the method using the improved ESH pyrolysis pyrogram was experimentally studied. The differences between the modified and basic approaches and the quality evaluation criterions for samples with different kerogen richness were obtained using the measured pyrolysis pyrograms. Essentially, the conclusion drawn from the present research would be summarized as follows:

1. The ESH cycle, which started at a lower temperature of 150°C with a lower heating rate of 10°C/min, proved to be trustworthy in evaluating the quality of the cleaning process of hydrocarbons in shale.
2. The targets in the cleaning process are the light free hydrocarbons and the FHR, but the kerogen and the solid bitumen should be excluded.
3. For the kerogen-rich shale, the cleaning of hydrocarbon is accomplished when S_A and S_B disappear and S_C stays almost unchanged on the modified ESH pyrogram.
4. The FHR that remained to the second stage of the Rock-Eval II cycle is the most significant difference between the modified ESH pyrogram and the basic Rock-Eval II pyrogram.
5. Using the modified pyrogram could improve the identification of production potential in shale reservoirs up to about 3% of the total pore volume.

ACKNOWLEDGMENT

This work was supported by the National Nature Science Foundation of China (41874152, 41804125) and the Natural Science Basic Research Program of Shanxi (2018JQ4043).

ORCID

Xu Dong https://orcid.org/0000-0002-2815-5851

REFERENCES

1. Sondergeld CH, Ambrose RJ, Rai CS, Moncrieff J. *Micro-Structural Studies of Gas Shales*. Pittsburgh, Pennsylvania, USA, 23-25 February, 2010; 2010. https://www.onepetro.org:443/conference-paper/SPE-131771-MS
2. Sondergeld CH, Newsham KE, Comisky JT, Rice MC, Rai CS. Petrophysical considerations in evaluating and producing shale gas resources. In: *SPE Unconventional Gas Conference held in Pittsburgh, Pennsylvania, USA, 23-25 February, 2010*; 2010. https://www.onepetro.org:443/conference-paper/SPE-131768-MS
3. Javadpour F, Moravvej Farshi M, Amrein M. Atomic-force microscopy: a new tool for gas-shale characterization. *J Can Pet Technol*. 2012;51(04):236-243.
4. Glorioso JC, Lolley R, Rattia AJ. A review of the fundamentals of shale gas evaluations: the dangers of effective porosity and clay excess conductivity corrections. In: *SPE/EAGE European Unconventional Conference and Exhibition, Vienna, Austria, 25-27 February 2014*; 2014.
5. Glorioso JC, Rattia A. Unconventional reservoirs: basic petrophysical concepts for shale gas. In: *SPE/EAGE European Unconventional Resources Conference and Exhibition, Vienna, Austria, 20-22 March 2012*; 2012.
6. Hook JR. An introduction to porosity. *Petrophysics*. 2003;44(3):205-212.
7. Kuila U, McCarty DK, Derkowski A, Fischer TB, Prasad M. Total porosity measurement in gas shales by the water immersion porosimetry (WIP) method. *Fuel*. 2014;117:1115-1129.
8. Sun J, Dong X, Wang J, et al. Measurement of total porosity for gas shales by gas injection porosimetry (GIP) method. *Fuel*. 2016;186:694-707.
9. Yao Y, Liu D, Che Y, Tang D, Tang S, Huang W. Petrophysical characterization of coals by low-field nuclear magnetic resonance (NMR). *Fuel*. 2010;89(7):1371-1380.
10. Dong X, Sun J, Li J, Gao H, Liu X, Wang J. Experimental research of gas shale electrical properties by NMR and the combination of imbibition and drainage. *J Geophys Eng*. 2015;12(4):610-619.
11. Stewart CR. *Cleaning Porous Media*. US Patents; 1952. US2617719 A. http://www.google.com/patents/US2617719
12. Conley FR, Burrows DB. A centrifuge core cleaner. *J Petrol Technol*. 1956;8(10):61-62.
13. API. *Recommended Practices for Core Analysis*. Washington, DC: American Petroleum Institute; 1998.
14. Sanei H, Wood JM, Ardakani OH, Clarkson CR, Jiang C. Characterization of organic matter fractions in an unconventional tight gas siltstone reservoir. *Int J Coal Geol*. 2015;150-151:296-305.
15. Golsanami N, Sun J, Liu Y, et al. Distinguishing fractures from matrix pores based on the practical application of rock physics inversion and NMR data: a case study from an unconventional coal reservoir in China. *J Nat Gas Sci Eng*. 2019;65:145-167.
16. Luffel DL, Guidry FK. New core analysis methods for measuring reservoir rock properties of Devonian shale. *J Petrol Technol*. 2013;44(11):1184-1190.
17. Passey QR, Bohacs K, Esch WL, Klimentidis R, Sinha S. From oil-prone source rock to gas-producing shale reservoir - geologic and petrophysical characterization of unconventional shale gas reservoirs. In: *CPS/SPE International Oil & Gas Conference and Exhibition in China held in Beijing, China, 8-10 June, 2010*; 2010.
18. Etminan SR, Javadpour F, Maini BB, Chen Z. Measurement of gas storage processes in shale and of the molecular diffusion coefficient in kerogen. *Int J Coal Geol*. 2014;123:10-19.
19. Tissot BP, Welte DH. *Petroleum Formation and Occurrence*. Berlin, Heidelberg, New York, Tokyo: Springer Verlag; 1985.
20. Carrie J, Sanei H, Stern G. Standardisation of Rock-Eval pyrolysis for the analysis of recent sediments and soils. *Org Geochem*. 2012;46:38-53.

21. Vandenbroucke M, Largeau C. Kerogen origin, evolution and structure. *Org Geochem*. 2007;38(5):719-833.
22. Kondla D, Sanei H, Clarkson CR, Ardakani OH, Wang X, Jiang C. Effects of organic and mineral matter on reservoir quality in a middle Triassic mudstone in the Canadian Arctic. *Int J Coal Geol*. 2016;153:112-126.
23. Li Y, Guo Z-Q, Liu C, Li X-Y, Wang G. A Rock physics model for the characterization of organic-rich shale from elastic properties. *Petrol Sci*. 2015;12(2):264-272.
24. Synnott DP, Dewing K, Ardakani OH, Obermajer M. Correlation of zooclast reflectance with Rock-Eval Tmax values within upper Ordovician cape Phillips formation, a potential petroleum source rock from the Canadian Arctic Islands. *Fuel*. 2018;227:165-176.
25. McCarthy K, Rojas K, Niemann M, Palmowski D, Peters K, Stankiewicz A. Basic petroleum geochemistry for source rock evaluation. *Oilfield Rev*. 2011;23(2):32-43.
26. Jin JM, Kim S, Birdwell JE. Molecular characterization and comparison of shale oils generated by different pyrolysis methods. *Energy Fuels*. 2012;26(2):1054-1062.
27. Baudin F, Disnar J-R, Aboussou A, Savignac F. Guidelines for Rock-Eval analysis of recent marine sediments. *Org Geochem*. 2015;86:71-80.
28. Deygout F. Volatile emissions from hot bitumen storage tanks. *Environ Prog Sustain Energy*. 2011;30(1):102-112.
29. Lo TC, Baird MH, Hanson C. *Handbook of Solvent Extraction*. Michigan: Krieger Publishing Company; 1983.
30. Jiang C, Chen Z, Mort A, et al. Hydrocarbon evaporative loss from shale core samples as revealed by Rock-Eval and thermal desorption-gas chromatography analysis: its geochemical and geological implications. *Mar Pet Geol*. 2016;70:294-303.
31. Chen Z, Liu X, Guo Q, Jiang C, Mort A. Inversion of source rock hydrocarbon generation kinetics from Rock-Eval data. *Fuel*. 2017;194:91-101.
32. Lafargue E, Marquis F, Pillot D. Rock-eval 6 applications in hydrocarbon exploration, production, and soil contamination studies. *Oil Gas Sci Technol*. 1988;53(4):421-437.
33. Haeseler F, Blanchet D, Druelle V, Werner P, Vandecasteele JP. Analytical characterization of contaminated soils from former manufactured gas plants. *Environ Sci Technol*. 1999;33(6):825-830.
34. Espitalie J, Marquis GDF. Rock-eval pyrolysis and its applications. *Oil Gas Sci Technol*. 1985;5:563-579.
35. Ordoñez L, Vogel H, Sebag D, et al. Empowering conventional Rock-Eval pyrolysis for organic matter characterization of the siderite-rich sediments of Lake Towuti (Indonesia) using end-member analysis. *Org Geochem*. 2019;134:32-44.
36. Disnar JR, Guillet B, Keravis D, Di Giovanni C, Sebag D. Soil organic matter (SOM) characterization by Rock-Eval pyrolysis: scope and limitations. *Org Geochem*. 2003;34:327-343.
37. HetÉnyi M, Nyilas T. Soil organic matter characterization using S3 and S4 signals from Rock-Eval pyrolysis. *Pedosphere*. 2014;24(5):563-574.
38. Fathi E, Akkutlu IY. Matrix heterogeneity effects on gas transport and adsorption in coalbed and shale gas reservoirs. *Transport Porous Med*. 2009;80(2):281-304.
39. Wang X, Zhang L, Chao G. The heterogeneity of lacustrine shale gas reservoir in Yanchang Formation, Xiasiwan Area, Ordos Basin. *Acta Geolog Sin - English Ed*. 2015;89(s1):99-101.
40. Liu X, Wang J, Ge L, et al. Pore-scale characterization of tight sandstone in Yanchang Formation Ordos Basin China using micro-CT and SEM imaging from nm- to cm-scale. *Fuel*. 2017;209:254-264.
41. Osborne MJ, Swarbrick RE. Mechanisms for generating overpressure in sedimentary basins: a reevaluation. *AAPG Bull*. 1997;81(6):1023-1041.
42. Bowker KA. Barnett shale gas production, Fort Worth basin: issues and discussion. *AAPG Bull*. 2007;91(4):523-533.
43. Cardott BJ, Landis CR, Curtis ME. Post-oil solid bitumen network in the Woodford Shale, USA — a potential primary migration pathway. *Int J Coal Geol*. 2015;139:106-113.
44. Środoń J, MaCarty DK. Surface area and layer charge of smectite from Cec and Egme/H_2O-retention measurements. *Clays Clay Miner*. 2008;56(2):155-174.

How to cite this article: Dong X, Shen L, Zhao J, et al. A novel method to evaluate cleaning quality of oil in shale using pyrolysis pyrogram. *Energy Sci Eng*. 2020;00:1–12. https://doi.org/10.1002/ese3.625